Synergistic effect of dicarbollide anions in liquid–liquid extraction: a molecular dynamics study at the octanol–water interface†

G. Chevrot, R. Schurhammer and G. Wipff*

Received 15th November 2006, Accepted 31st January 2007
First published as an Advance Article on the web 23rd February 2007
DOI: 10.1039/b616753e

We report a molecular dynamics study of chlorinated cobalt bis(dicarbollide) anions $[(B_9C_2H_8Cl_3)_2Co]^-$ "CCD^-" in octanol and at the octanol–water interface, with the main aim to understand why these hydrophobic species act as strong synergists in assisted liquid–liquid cation extraction. Neat octanol is quite heterogeneous and is found to display dual solvation properties, allowing to well solubilize CCD^-, Cs^+ salts in the form of diluted pairs or oligomers, without displaying aggregation. At the aqueous interface, octanol behaves as an amphiphile, forming either monolayers or bilayers, depending on the initial state and confinement conditions. In biphasic octanol–water systems, CCD^- anions are found to mainly partition to the organic phase, thus attracting Cs^+ or even more hydrophilic counterions like Eu^{3+} into that phase. The remaining CCD^- anions adsorb at the interface, but are less surface active than at the chloroform interface. Finally, we compare the interfacial behavior of the $Eu(BTP)_3^{3+}$ complex in the absence and in the presence of CCD^- anions and extractant molecules. It is found that when the CCD^-'s are concentrated enough, the complex is extracted to the octanol phase. Otherwise, it is trapped at the interface, attracted by water. These results are compared to those obtained with chloroform as organic phase and discussed in the context of synergistic effect of CCD^- in liquid–liquid extraction, pointing to the importance of dual solvation properties of octanol and of the hydrophobic character of CCD^- for synergistic extraction of cations.

Introduction

The chlorinated cobalt bis(dicarbollide)s $[(B_9C_2H_8Cl_3)_2Co]^-$ (hereafter noted CCD^-) belong to a class of bulky "peanut-shaped" anions[1] that are used in conjunction with extractant molecules for efficient liquid–liquid extraction of cations.[2] The anions can be used as such (generally introduced as their Cs^+ CCD^- or H_3O^+ CCD^- salts in the organic phase),[3–9] or grafted onto complexing moieties (phosphoryl containing ligands, glycols), sometimes anchored on organized platforms like calixarenes or cavitands.[10,11] Due to their very high hydrophobicity, high chemical and radiochemical stability, and the extreme acidity of the conjugated acid, dicarbollides display great potentials in the field of nuclear waste partitioning from highly acidic aqueous solutions. Important applications involve the removal of Cs^+ and Sr^{2+} cations, or the extraction of trivalent actinide and lanthanide M^{3+} cations,[10–14] generally leading to significant extraction enhancement. For instance, Eu^{3+} is extracted by CMPO-cavitands from water to *o*-nitrophenyl hexyl ether, and the distribution coefficient D_{Eu} increases from 16.7 to more than 100 at $[HNO_3]$ = 0.001 M or from 0.86 to more than 100 at $[HNO_3]$ = 1 M upon addition of CCD^-'s.[9] Due to their weak solubility in aliphatic solvents (alkanes, kerosene) and their halogenated derivatives (*e.g.* chloroform),[15] CCD^-'s are generally dissolved in aromatic solvents (*e.g.* nitrobenzene or ester derivatives, alkylbenzenes) or in fluorinated solvents, thereby raising environmental issues. More recent experiments have been carried out with octanol as organic phase, and significant Am^{3+}/Eu^{3+} partitioning was observed with the nitrogen based BTP ligands used with a synergistic mixtures of CCD^- anions, and CMPO molecules (sketched in Fig. 1).[16]

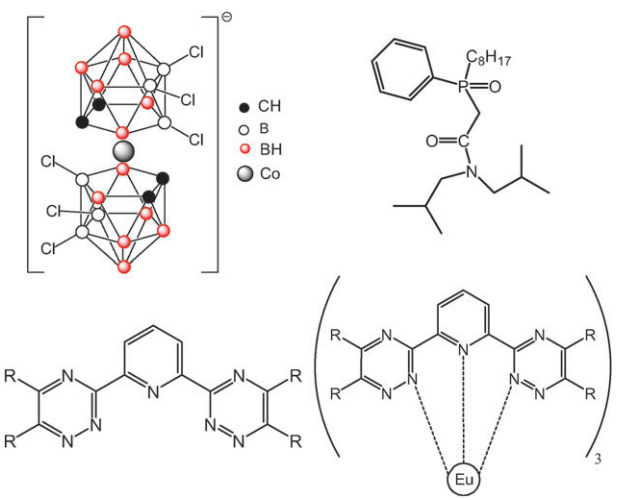

Fig. 1 CCD^-, CMPO ((*N*,*N*-diisobutylcarbamoylmethyl)octylphenylphosphine oxide), BTP (2,6-bis(5,6-isopropyl-1,2,4-triazin-3-yl)-pyridine; R = *i*-Pr) and the $Eu(BTP)_3^{3+}$ complex.

Laboratoire MSM, UMR CNRS 7177, Institut de Chimie, Université Louis Pasteur, 4, rue B., 67 000 Strasbourg, France. E-mail: wipff@chimie.u-strasbg.fr

† Electronic supplementary information (ESI) available: Experimental details and snapshots of the octanol solutions and interfaces. See DOI: 10.1039/b616753e

What happens at the nanoscopic level in such heterogeneous complex systems is presently unknown and of key importance for the understanding of other processes involving biphasic systems, like the partitioning of drugs,[17] phase transfer catalysis,[18] interfacial electrochemistry[19] or environmental issues. This led us to recently initiate molecular dynamics "MD" studies on the behavior of CCD^- anions and their derivatives in chloroform, water and at the chloroform–water interface, where interesting aggregation phenomena were observed.[20] In this paper, we extend these studies on aqueous interfaces, focusing on octanol as organic phase. Furthermore, we address the question of synergistic effect of CCD^- upon extraction of trivalent lanthanide or actinide cations, selecting the recently developed nitrogen bearing BTP 2,6-bis(5,6-isopropyl-1,2,4-triazin-3-yl)pyridine ligands,[21–24] focusing on the interfacial distribution of key partners. Octanol is an interesting protic medium based on amphiphilic molecules, and it will be interesting to see how these interact with soft delocalized anions like CCD^- and with their counterions. Octanol can be used as receiving phase[25] as well as additive to organic solvents ("solvent modifier") in liquid extraction.[26–29] The octanol/water partition coefficients log $P_{octanol}$[30] are also important indicators of the bioavailability of potential drugs[31] or of the transport of pollutants in soil–water systems.[32,33] On the computational side, there are several reports of MD studies on the neat octanol liquid and of its interactions with water,[34–40] and of the octanol–water interface either neat[41] or in the presence of spectroscopic probes.[42–45] These studies point to the heterogeneous structure of octanol, comprising apolar and polar domains, thus allowing for dual specific interactions with hydrophobic, heterogeneous solutes. When compared to organic solvents like aromatic derivatives where CCD's are soluble, octanol also displays interesting amphiphilic features, thus forming layers or bilayers at aqueous interfaces. It will thus be interesting how these interact with CCD^- salts and with complexed metals.

More specifically, we report a MD study of the CCD^- Cs^+ salt in octanol solutions and in water–octanol binary mixtures, in order to gain insight into its solvation patterns, the nature of the ion pairs, and the possible supramolecular arrangements (aggregation). As a reference, we first report our results on the octanol–water binary system. We then study concentrated solutions of CCD^- Cs^+ salts in octanol and in biphasic octanol–water solutions. They are compared at the interface with their analogues involving the more hydrophilic Eu^{3+} cations, in order to explore how these ions partition, to what extent they are surface active, and how they are solvated. Most simulations will be carried out with *ca.* 50 : 50 volume ratios of water : octanol, but 90 : 10 mixtures will also be considered in order to model oil-rich mixtures that gradually form in extraction experiments. The final part of the paper concerns the synergistic effect of CCD^- upon the Eu^{3+} extraction by BTP molecules. For this purpose, the $Eu(TBP)_3^{3+}$ complex will be simulated in water–octanol mixtures in the presence of other extractant molecules, with and without CCD^-, with the aim to investigate "what happens at the interface"[46] and to understand why the CCD^-'s promote the extraction of trivalent cations (and a fortiori of less hydrophilic mono- and divalent cations) to an hydrophobic alcohol phase. The comparison of selected interfacial systems with chloroform, instead of octanol as organic phase will provide further insight into the role of the receiving phase in liquid extraction.

Methods

Molecular dynamics simulations were performed with the AMBER 7.0[47] software based on the following representation of the potential energy U:

$$U = \sum_{\text{bonds}} K_l(l - l_0)^2 + \sum_{\text{angles}} K_\theta(\theta - \theta_0)^2 + \sum_{\text{dihedrals}} \sum_n V_n(1 + \cos(n\varphi - \gamma)) + \sum_{i<j} \left(\frac{q_i q_j}{R_{ij}} - 2\varepsilon_{ij}\left(\frac{R^*_{ij}}{R_{ij}}\right)^6 + \varepsilon_{ij}\left(\frac{R^*_{ij}}{R_{ij}}\right)^{12} \right)$$

It accounts for the deformation of bonds (l), angles (θ), dihedral angles (φ), and for electrostatic and van der Waals interactions between non-bonded atoms. For the CCD^- anions, the reference l_0 bond lengths and θ_0 angles were taken from experiment[48] and the charges have been derived from HF/3-21G* calculations.[49] These charges give similar results as those derived from B3LYP/6-31G* calculations.[20]

The charges of BTP and the $Eu(BTP)_3^{3+}$ complex were obtained from DFT(B3LYP)/6-31G* optimized structures, using a large core ECP and the affiliated (7s6p5d)/[5s4p3d] basis set basis for Eu^{3+}.[50,51] The charges of the free BTP ligand were derived from electrostatic potentials using the Merz-Kollman procedure implemented in Gaussian03.[52] For the $Eu(BTP)_3^{3+}$ complex we used the Mulliken charges that better reflect polarization and charge transfer. The CMPO parameters are from ref. 53. The charges and AMBER atom types of the CCD^-, BTP, $Eu(TBP)_3^{3+}$, CMPO and NO_3^- species are given in Fig. S1.† The Lennard-Jones parameters of the Cs^+,[54] and Eu^{3+} [55] cations were fitted on their free energies of hydration.

The solvents were represented explicitly at the molecular level, using the TIP3P model[56] for water, and by the DeBolt and Kollman's model for octanol[34] where CH_n groups are represented with united atom models. Typical snapshots of the simulated octanol liquid can be seen in Fig. S2.† Non bonded interactions were calculated with a 12 Å atom based cut-off, correcting for the long-range electrostatics by using the Ewald summation method (PME approximation). The solutions were simulated with 3D-periodic boundary conditions, thus as alternating slabs of water and "oil" in the case of biphasic systems.

The interface was built from adjacent boxes of water and octanol as in ref. 57. The solutions contain 30 CCD^- anions neutralized by either 30 Cs^+, or 10 Eu^{3+} cations, corresponding to a concentration of 0.2 mol L^{-1}, which is close to the concentration used in extraction experiments.[4] After 1000 steps of energy minimization, we performed 50 ps of MD with fixed solutes ("BELLY" option of AMBER) and 50 ps without constraints, followed by 50 ps at a constant pressure of 1 atm (monitored with a weak coupling method[58]). The production stage was performed at 300 K in the (NVT)

ensemble for at least 2 ns. The temperature was maintained constant by coupling the solution to a thermal bath using the Berendsen algorithm[58] with a relaxation time of 0.2 ps. The main characteristics of the simulated systems are summarized in Table S1.†

The coordinates were saved every 1 ps, and analysed using the MDS and DRAW software.[59] Some snapshots were redrawn with the VMD software.[60] The position of the interface was dynamically defined as the intersection between the water and oil density curves.[61] Defining the width of the interface is somewhat arbitrary and the latter was defined as the z-distance between the points where the solvent densities reach 90% of their "bulk" experimental values, averaging over the two oil–water interfaces. The percentage of ions "at the interface" was calculated during the last 0.75 ns, selecting the species that are within 10 Å from the interface. We defined the density of solvents and solutes (g cm^{-3}) at a z-position by their mass per volume unit ($dv = xy\,dz$). The ion–ion and ion–solvent interactions were characterized by the radial distribution functions (RDFs) calculated during the last 0.25 ns. The average coordination numbers (noted CN) were obtained by integration of the first peak of the RDFs. The diffusion coefficient D, was calculated from the Einstein equation:[62] $D = \frac{1}{6}\lim_{t\to\infty}\frac{d}{dt}\langle|r_i(t) - r_i(0)|^2\rangle$ over the last nanosecond of dynamics, where $r_i(t)$ is the position of atom i at time t. The orientation of the octanol molecules at the interface was defined by the angle θ between the z-axis (perpendicular to the interface) and the C–O vector connecting their terminal CH_3 and oxygen atoms. The corresponding order parameter S, defined as $S = 0.5\,\langle(3\cos^2\theta - 1)\rangle$ would range from 1.0 if the molecules were perfectly ordered perpendicular to the interface, to −0.5 if they were parallel.

Results

We first present the main characteristics of octanol–water mixtures simulated in different conditions. This is followed by the distribution of CCD^- salts in pure octanol and at the octanol–water interface, comparing Cs^+ to Eu^{3+} as counter-ions at the interface. The last section deals with the synergistic effect of CCD^- anions upon extraction of the $Eu(BTP)_3^{3+}$ complex, focusing on the interfacial landscape and distribution of the complex and CCD^-'s at the interface.

I Neat octanol–water binary systems

In this section, we describe octanol–water binary mixtures and the corresponding interface, depending on the way it has been prepared (relaxation of juxtaposed liquids *versus* phase separation of completely mixed liquids), and also somewhat on the shape of the simulation box (see Fig. 2 for the 50 : 50 mixture and Fig. 3 for the 90 : 10 and 10 : 90 mixtures).

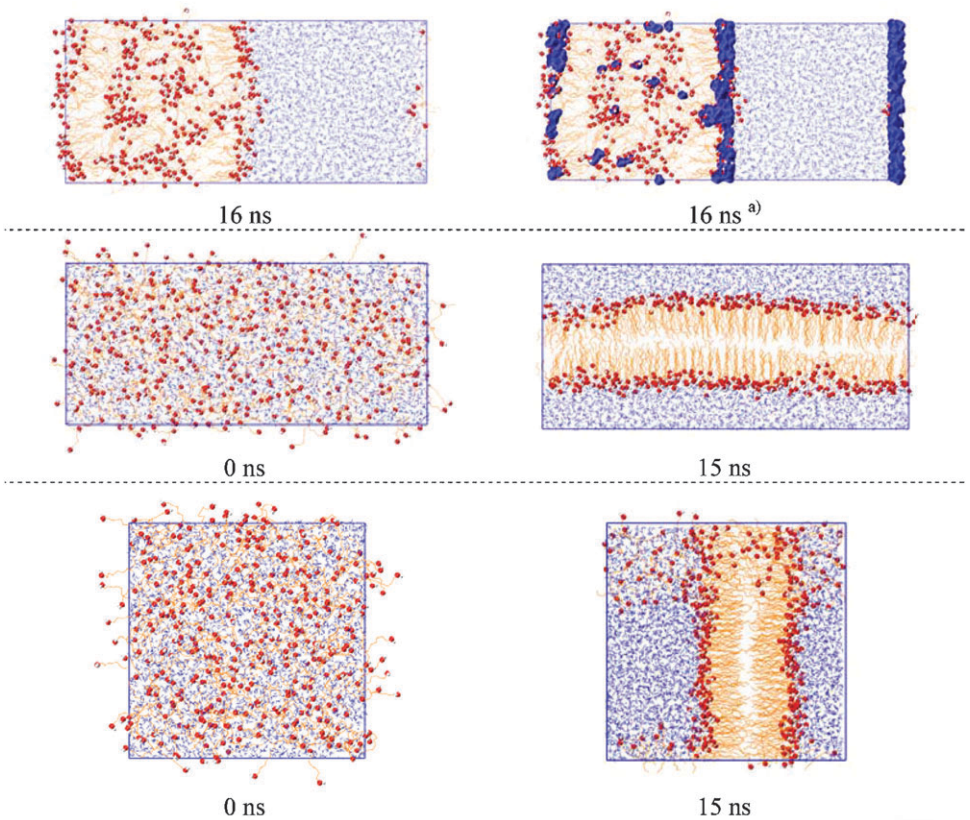

Fig. 2 Octanol–water 50 : 50 mixtures simulated from juxtaposed liquids, from mixed liquids in a "rectangular" box and from mixed liquids in a cubic box. Snapshots taken along the demixing simulations are given in Fig. S5.† (a) H_2O molecules in octanol and at the interface are highlighted in dark blue color.

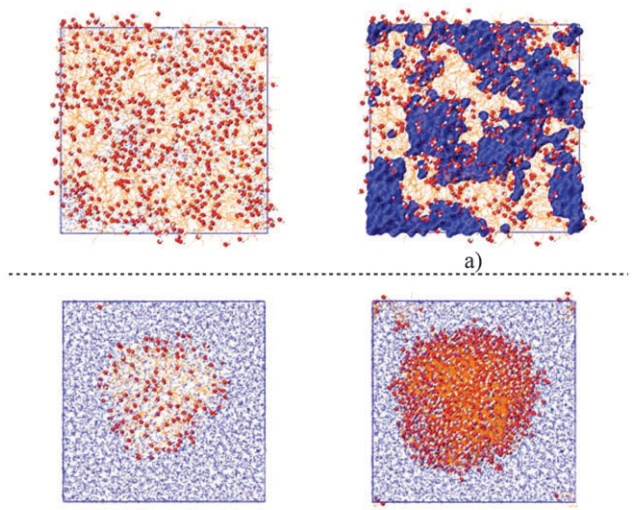

Fig. 3 Octanol–water mixtures at 90 : 10 (top) and 10 : 90 ratio (bottom). Final configurations (at 5 ns) of the "demixing simulations". (a) H_2O molecules are highlighted in dark blue color.

1. The octanol–water interface between juxtaposed liquids

Solvent mixing. In the simulation that started with juxtaposed "cubic" solvent boxes, the octanol and water phases remained well distinct and separated by an interface. After 15 ns of dynamics, no octanol is found in water, which is consistent with the corresponding low experimental solubility (4.4×10^{-5} in mole fraction[63]). The "bulk" octanol phase is somewhat "humid", and its water content is quite constant during the last 10 ns (Fig. S3†), indicating that the system is equilibrated. In octanol beyond 5 Å from the interface, one finds a molar fraction of water of *ca.* 0.05, which is much lower than the experimental value of 0.27 obtained with water-saturated octanol.[63] Considering all water molecules that sit between the two Gibbs dividing surfaces gives a molar fraction of 0.21, still lower than the experimental value. The difference may arise from the fact that, in our simulations, the water molecules are diluted in octanol in the form of monomers or dimers H-bonded to octanol molecules (Fig. S4†), without forming higher aggregates or "water pockets". Experimentally, however, such patterns cannot be precluded, leading to a higher water content.[64]

Shape and width of the interface. The interface is quite narrow (*ca.* 5.5 Å; see Fig. S3†) and comparable to the chloroform–water interface (≈7 Å),[61] but narrower than the aqueous interfaces with hydrophobic ionic liquids like [BMI][PF_6] or [BMI][Tf_2N] (≈10 Å).[65,66] Note that the interface is not "flat" and can be instantaneously quite rough, with water protuberances of *ca.* 10 Å penetrating into octanol (Fig. 2).

Orientation of octanol at the interface. Octanol molecules are isotropically oriented in the bulk octanol domain (the order parameter is $\langle S \rangle \approx 0.0$), but not at the interface ($\langle S \rangle \approx 0.6$). As seen by the distribution $p(\theta)$ in Fig. S3,† they are not strictly perpendicular, but rather tilted (by *ca.* 30 to 40°, on average) at the interface, as found by other calculations[41,44,45] and by spectroscopic techniques.[31,67,68] We also notice that the octanol density fluctuates along the *z*-direction in the bulk domain (Fig. 2), which corresponds to enriched and depleted zones, as observed by Napoleon and Moore.[41] The lack of such irregularities in the neat octanol liquid simulated in consistent conditions (see Fig. S2)† clearly indicates that they result from the strong ordering of the octanol molecules at the interface, inducing bilayer type assembling (*vide infra*).

Concerning the orientation of water molecules, defined by the θ angle between the *z*-axis and their two protons, one finds $\langle S \rangle$ close to zero in the entire box, showing that the water molecules are isotropically oriented at the interface as in the bulk.

Specific interactions with water at the interface. The OH heads of octanol pointing towards the aqueous phase form hydrogen bonds with water and other octanol molecules. A perspective snapshot is shown in Fig. S4.† Selecting all alcohol groups that sit within 5 Å from the interface one finds 0.8 O_{H_2O} per H_{oct} and 1.1 H_{H_2O} per O_{oct}, on average. There are also a few H-bonds between hydroxyl groups (0.2 O_{oct} per H_{oct} and 0.2 H_{oct} per O_{oct}, which is less than in pure octanol). Thus, as found in previous simulations,[41–45] octanol molecules preferentially interact with water rather than other octanol molecules at the interface.

2. Demixing simulation of "randomly mixed" octanol–water liquids

When the octanol–water randomized mixture was simulated by MD, the two components separated in *ca.* 8 ns. This is much slower than in the case of the chloroform–water mixture (0.5 ns),[57] in conjunction with the higher viscosity[40] and lower diffusion coefficient of octanol, compared to chloroform.[69] The dynamics was pursued up to 15 ns and, interestingly, the resulting system differed from the one obtained from juxtaposed liquids (Fig. 2 and S5†). The demixing simulation indeed leads to the formation of a well-defined octanol bilayer where the two hydrocarbons tails of each layer overlap. As the bilayer is quite elongated, we speculated that this particular structure resulted from the "rectangular" shape of the simulation box, thereby favoring the formation of interfaces. We therefore repeated the mixing–demixing simulation in a cubic box of identical volume, with the same number of particles. The phase separation again resulted in the formation of a single bilayer, somewhat less regular however. Because the interfacial area is *ca.* 1.3 times smaller in the cubic than in the "rectangular" box, a few octanol molecules remain in the water phase of the cubic box. Similar bilayers have been observed by Lambert and Sum in MD "demixing" simulations of an octanol–water mixture where octanol is represented using an all-atom model.[45] When they used an united model, however these authors found different octanol patterns, where a humid octanol slab is inserted between the two interfacial layers.[45] On the other hand, using a somewhat different protocol, box size and composition, Napoleon and Moore observed more complex arrangements beyond the interface,[41] as found in our simulation of juxtaposed liquids, illustrating the versatile structure of octanol in confined conditions. It

should be recalled that, because all simulated solutions have been represented with 3D-periodic boundary conditions, none really corresponds to a biphasic solution, *i.e.* to a single interface between "infinite" aqueous and octanol phases. One simulates in fact alternating thin "vertical" slabs of liquids in the case of juxtaposed liquids, and more complex alternations of water and octanol (bi)layers in the case of the phase separation. Further insight into the octanol structure beyond the interface would require using bigger solvent boxes, and hence presently prohibitive computer costs for our study with CCD's (*vide infra*).[70] Comparing the relative total potential energies of demixed and juxtaposed rectangular boxes, and of the demixed cubic box one finds 0, 650 and 150 kcal mol^{-1}, respectively, which suggests that the elongated bilayer structure is the most stable one from an enthalpic point of view. In the latter, the octanol molecules indeed optimize their mutual packing interactions and their interactions with water, and there is no water inside the hydrophobic core of the layer(s). On the other hand, systems with octanol bilayers should be somewhat penalized from an entropic point of view.

3. Demixing simulations of mixtures with 90 : 10 and 10 : 90 octanol–water mixtures

In liquid–liquid extraction experiments, the two phases are stirred and locally, one solvent may be in excess over the other. We thus examined mixtures corresponding to octanol : water ratio 90 : 10 and 10 : 90, respectively, where solvent molecules were initially randomly mixed. After 5 ns of demixing simulation, when octanol is in excess, water is dispersed in the form of small aggregates or clusters (see Fig. 3), onto which the OH heads of octanols adsorb. Conversely, when water is in excess, the amphiphilic character of octanol is manifested by the formation of a spherical micelle where hydrophilic OH groups point outside and are solvated by water molecules, whereas octyl tails are attracted inside by solvophobic forces.

II Dicarbollide salts in octanol and at the octanol–water interface

We now turn to the study of 30 CCD^-, Cs^+ ions immersed in an octanol solution, and compare their distribution to those observed in chloroform and in water.[20] We also examine their distribution in binary solutions of 50 : 50 and 90 : 10 octanol–water ratio, respectively. In order to assess the role of the counterions, we also simulate the 30 CCD^-'s with Eu^{3+}, instead of Cs^+ counterions in the 50 : 50 solution.

1. CCD^-, Cs^+ salts in an octanol solution

When the 30 CCD^-, Cs^+ ions were simulated for 5 ns in pure octanol they got diluted, however retaining loose contacts between cations and anions (Fig. 4). This distribution is thus quite different from those observed in chloroform or water solutions where the CCD^-'s aggregate, in the form of a neutral droplet and of an anionic cluster, respectively.[20] In octanol, each Cs^+ cation is surrounded by 1.8 Cl_{CCD} atoms of the anions plus 4.0 octanol oxygens, on average. The Cs^+ cations and CCD^- anions do not form single ion pairs, but rather oligomers of alternating anions and cations (see a snapshot in Fig. 4). The solvation of the CCD^- anions by octanol does not involve H-bonds with the hydroxylic proton, in conjunction with the high acidity of CCD^-, but rather van der Waals contacts of the alkyl moieties, in conjunction with the marked hydrophobic character of the anions. This is an interesting feature if one refers to the quasi insolubility of CCD^- in aliphatic solvents or in chloroform. In fact, the interaction energy E_{solv} between one CCD^- and octanol (−50 kcal mol^{-1}) is somewhat stronger that its interaction with chloroform (−42 kcal mol^{-1}), and van der Waals contributions (51 and 40%, respectively) are higher in the former liquid. Another contribution to the higher solubility in octanol likely stems from the counterion (Cs^+, H_3O^+) that is better solvated by the polar

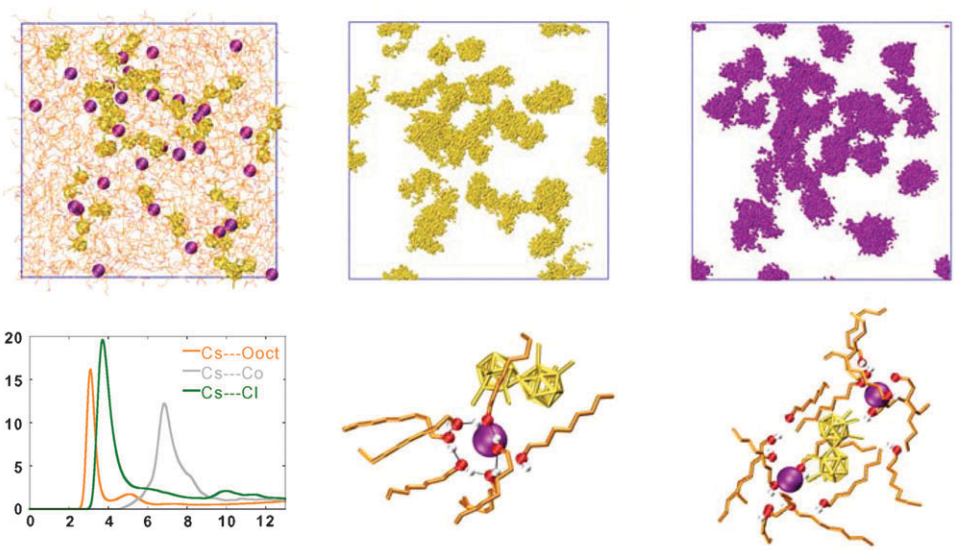

Fig. 4 Octanol solution of 30 CCD^- Cs^+ ions. From top left to bottom right: final snapshot (at 5 ns), cumulated positions of Co(CCD) (yellow) and Cs atoms (purple) during the last ns, RDF's around the Cs atom, and typical solvation of Cs^+ and CCD^- ions.

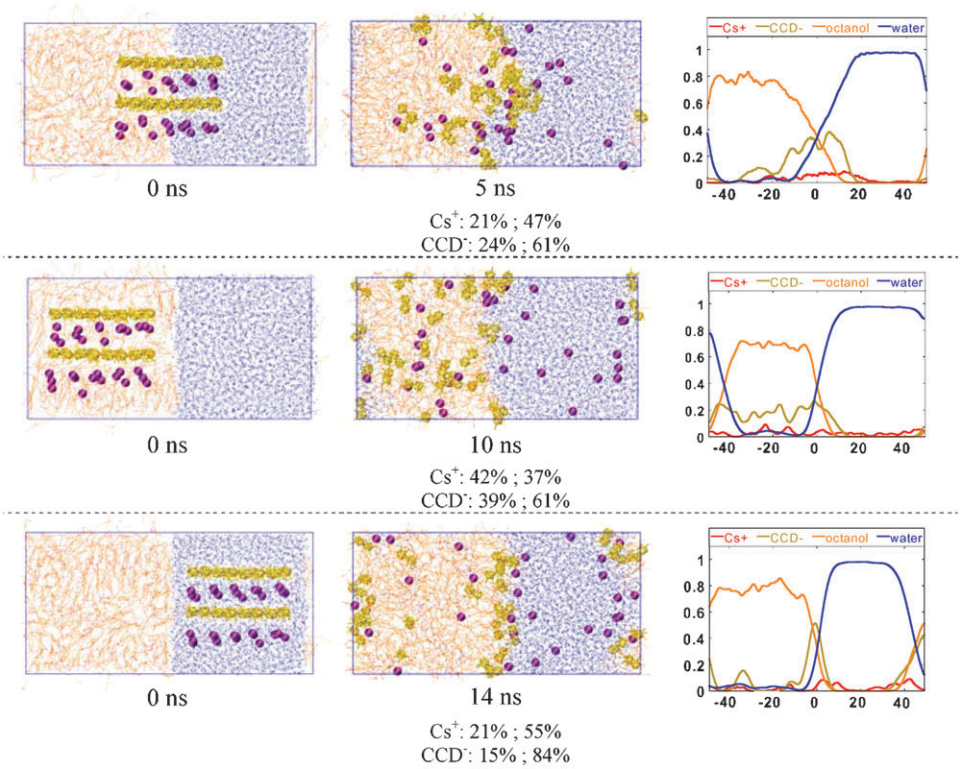

Fig. 5 30 CCD^- Cs^+ ions at the octanol–water interface, simulated with the ions initially at the interface (top), in octanol (middle), or in water (bottom). Initial and final views, and average densities as a function of the *z*-position. Percentage of Cs^+ and CCD^- ions in "bulk" octanol and within 10 Å from the interface. The corresponding electrostatic potentials are given in Fig. S6.†

heads of alcohols than by, *e.g.*, chloroform of aliphatic solvents.

An important feature of the octanol solution is the slow dynamics of the ions, illustrated by cumulated views over the last ns (Fig. 4). The CCD^- and Cs^+ ions are trapped in micro-domains and are much less mobile in octanol than in water or in chloroform. Their diffusion coefficients D (in 10^{-7} cm^2 s^{-1} units) are 6 and 8, respectively, in octanol, and 56 and 317, respectively, in water, indicating that the mobility is more reduced for Cs^+ than for CCD^- ions when one moves from water to octanol. In fact, in water, the majority of Cs^+ cations are hydrated without direct contact with the anions, whereas in octanol they are "anchored" to the OH octanol heads and to the CCD^- counterions. As a result, they diffuse even more slowly in octanol than in chloroform (D_{CCD^-} = 10.10^{-7} and D_{Cs^+} = 9.10^{-7} cm^2 s^{-1}) where they collapse to form a single droplet.[20]

2. CCD^-, Cs^+ ions at octanol–water interface

The 30 CCD^-, Cs^+ ions were simulated at the octanol–water interface, starting with a grid of 4 × 15 ions at three different initial positions, *i.e.* either "at the interface", or in octanol, or in water (see Fig. 5). The final distributions after 5–14 ns somewhat depend on the starting positions, due to the slow diffusion of CCD^- and Cs^+ in octanol. However, the three systems show some common features. There is no CCD^- anion in water, in conjunction with its high hydrophobic character. The majority of anions (more than 50%) are concentrated at the interface and the others (15 to 40%) are distributed in the bulk octanol. About one third of the Cs^+ cations sit in water, while the others are mainly concentrated at the interface or in octanol (68 to 79%). Interestingly, even in the simulation that started with all ions in water, the CCD^- anions attract the majority of cations at the interface and also extract some Cs^+ cations from water to the bulk octanol phase. We note that CCD^-'s are less surface active than they are at the chloroform–water interface,[20] because some migrate to the octanol phase, while none migrate to the chloroform phase where they are poorly soluble.[15]

The "bulk" octanol phase is overall quasi neutral, as it contains a similar proportion of Cs^+ cations and CCD^- anions (from *ca.* 20–40%, depending on the initial state; see Fig. 5), but the interface and the water phase are not neutral: Cs^+ cations are in excess over CCD^- anions in water, while CCD^- are in excess at the interface, creating a negative electrostatic potential, ϕ, on the octanol side of the interface and a positive potential, ϕ, on the water side (see Fig. S6).† Note that the total potential, ϕ, results from antagonistic contributions of the ions and of the solvent.

As seen by the RDFs (see Fig. S7)† and the resulting coordination numbers (CN) (see Table S2),† the Cs^+ cations are always hydrated and their hydration number depends on their position with respect to the interface, and on time. The Cs^+ hydration number progressively diminishes when one moves from the water phase (9 H_2O molecules) to octanol (from 2 to 5 H_2O, see Fig. S8).† We note that a similar

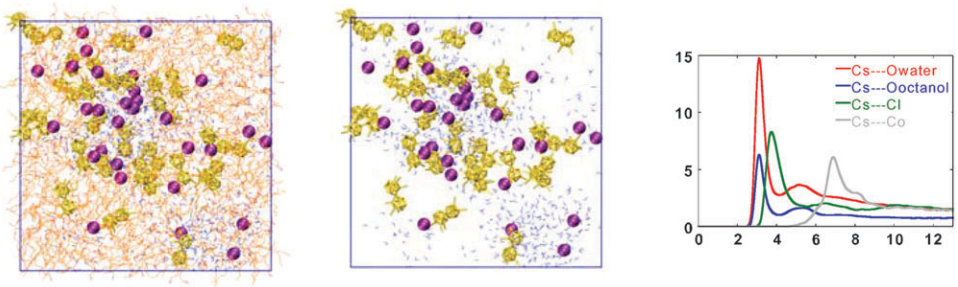

Fig. 6 30 CCD^- Cs^+ ions simulated in a 90 : 10 octanol–water mixture. Final snapshots (at 5 ns) with the two liquids (left), with octanol hidden for clarity (center), and RDF's around Cs^+ atoms (right).

reduction of ion hydration has been observed upon the simulated transfer of Na^+ and Cl^- ions across the related hexanol–water interface.[71] Concerning the solvation of Cs^+ by octanol, the corresponding CN is close to zero near the interface and reaches a maximum of 5 in the octanol phase. Regarding the $Cs^+ \cdots CCD^-$ interactions and contacts, they are more pronounced in the interfacial region than in the bulk octanol phase, because the anions are more concentrated at the interface.

It is interesting to follow the migration of a Cs^+ cation from water to octanol in the simulation that started with all ions in water. Typical snapshots are displayed in Fig. S9.† Initially, Cs^+ sits on the water side of the interface and is fully hydrated, without any contact with anions. In a second step (7.4–7.5 ns), Cs^+ is attracted by the anions at the interface where part of its hydration shell is displaced by octanol and CCD^-'s. In a third step (7.5–7.75 ns), the CCD^- anions lose the contact with the aqueous phase while Cs^+ is further dehydrated and migrates to the octanol side, solvated by octanol, H_2O molecules and CCD^- anions. Once in the octanol phase, Cs^+ coordinates to one labile H_2O molecule only, and to five octanol molecules, but not to CCD^- anions which are dissociated. The latter thus clearly promote the migration of Cs^+ cations *via* electrostatic attractions, without being necessarily paired.

3. CCD^-, Cs^+ ions in the oil-rich water mixtures

In order to mimic intermediate stages in macroscopic phases separation, we prepared a cubic box of a biphasic octanol-rich solution (90 : 10 octanol:water ratio), with 30 CCD^-, Cs^+ ions initially in the octanol phase. During the dynamics, the small water slab rearranged to form water droplets where the majority of Cs^+ cations solubilized (Fig. 6). The other cations are finally diluted in the octanol phase, solvated partially by water. Some CCD^- anions adsorb at the surface of water droplets, while others are diluted in octanol. The Cs^+ environment is, on average, quite similar to the one observed in the 50 : 50 octanol–water mixture where the salts were also initially in the organic phase (Table S2).† The main difference is that Cs^+ is somewhat less hydrated in the octanol-rich solution (4.8 O_{H_2O} *vs.* 5.8 O_{H_2O}), and thus interacts somewhat more with octanol and CCD^- species, as expected.

When the same solute was simulated in an analogous chloroform–water 90 : 10 mixture, the water molecules collapsed to a single droplet[20] instead of forming smaller aggregates, which is consistent with the higher hygroscopic character of octanol, compared to chloroform, and with its better solvation properties towards Cs^+ ions.

4. CCD^-, Eu^{3+} ions at octanol–water interface

As seen above, counterions play a major role in the solubility of CCD^- in octanol and in its surface activity, and we wondered whether highly hydrophilic cations like Eu^{3+} could still partition to the octanol phase. For this purpose, we simulated for 20 ns a binary solution containing 30 CCD^- plus 10 Eu^{3+} ions initially placed in the aqueous phase. The final distribution is quite surprising, as only 20% of the Eu^{3+} cations remained in the aqueous phase, whereas *ca.* 50% concentrated at the interface and 30% migrated to octanol (Fig. 7 and Fig. S10†). The driving force is clearly their attraction by the CCD^-'s in octanol or near the interface. Indeed, at the end of the simulation, all anions have been driven out of the water, the majority (72%) are adsorbed at the interface and the others are diluted in octanol. In all cases, the Eu^{3+} cations are fully hydrated by 9 H_2O molecules in their first shell. In octanol, their second shell is also mainly

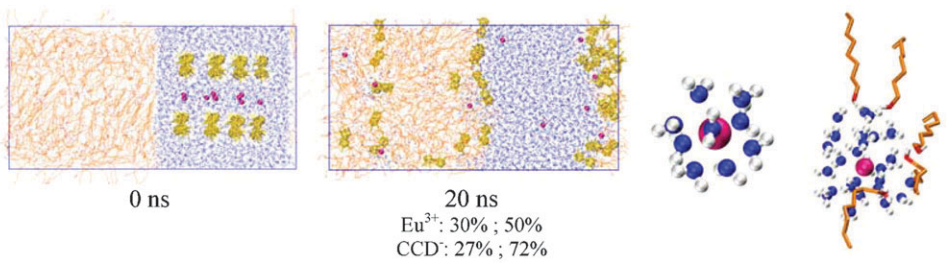

Fig. 7 30 CCD^- and 10 Eu^{3+} ions at the octanol–water interface, simulated with the ions initially in water. Initial and final views, with a zoom on the hydrated $Eu(H_2O)_n^{3+}$ complex extracted to octanol. The corresponding density profiles and electrostatic potentials are given in Fig. S10.†

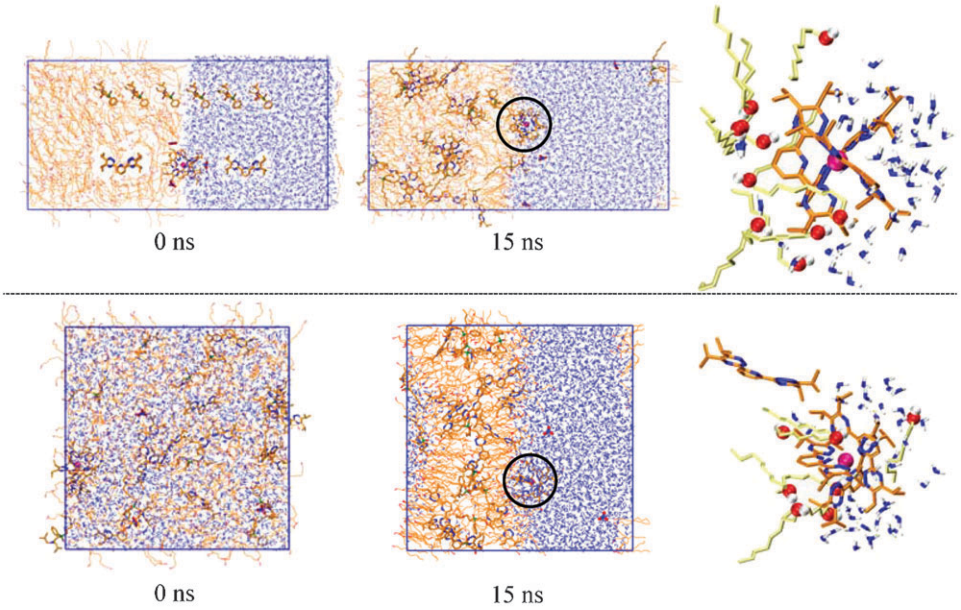

Fig. 8 The $Eu(BTP)_3^{3+}$, 3 NO_3^- complex in the presence of 12 CMPO and 12 BTP ligands at the octanol–water interface, simulated from juxtaposed liquids (top) and from mixed liquids (bottom). Initial and final views, with typical snapshots of the $Eu(BTP)_3^{3+}$ complex adsorbed at the interface.

constituted of water molecules, completed by some octanol molecules (4.4 on average), while CCD^- anions sit in the third shell or even farther, thus more remote from the cation than in the case of the CCD^- Cs^+ salt. There are 3 neutralizing CCD^-'s within 14 Å from Eu^{3+}, on average (Fig. S11).† Thus, in spite of the higher attractions of CCD^- with Eu^{3+}, compared to Cs^+, there is no ion pairing with the former, due to the strong solvation of Eu^{3+} by water molecules.

Comparing the amount of CCD^- ions at the interface, it was found to be higher for Eu^{3+} than for Cs^+ counterions. This is fully consistent with the known counterion effect on the stabilization of anionic micelles, whose critical micellar concentration (cmc) is lower with +3 charged than with +1 charged counterions.[72,73]

If one follows the migration of a selected Eu^{3+} ion from the water to the octanol phase during the dynamics (see Fig. S11),† one can see that the extraction "mechanism" is similar to the one observed with Cs^+, the main difference being that Eu^{3+} migrates as fully hydrated species, without any direct contact with the CCD^- anions. When Eu^{3+} approaches the interface, some octanol molecules displace H_2O molecules in the second or third shell, and the cation migrates in the form of a big $Eu(H_2O)_n^{3+}$ aggregate ($n \approx 30$ to 40),[74] progressively surrounded by octanol and CCD^-'s, thereby impeding the contact with the aqueous phase. The long range and medium range interactions with the CCD^-'s are thus crucial for directing the cation towards the interface and the oil phase, and these also "catalyze" the extraction of the complexed cation (*vide infra*).

III Extraction of the $Eu(BTP)_3^{3+}$ complex to octanol: synergistic effect of dicarbollide ions at the interface.

We investigated the behavior of the $Eu(BTP)_3^{3+}$ complex in "oil"–water biphasic systems, where the oil phase is octanol and, in some cases, chloroform, with the main aim to understand under which circumstances the complex is extracted to the oil phase. To the complex were added different combinations of free BTP ligands, of other extractant molecules like CMPO that are known to also extract trivalent lanthanides and actinides,[11,12,14] plus CCD^- ions with H_3O^+ as counterions. It will be shown that the latter, in large amounts, promote the extraction in conditions where the complex is otherwise not extracted. Since the Eu^{3+} cation achieves a nine coordination to the complexed BTP ligands, it is well shielded and was simulated with 3 NO_3^- dissociated counterions, initially positioned at *ca.* 10 Å.

1. On the high surface activity of the $Eu(BTP)_3^{3+}$ complex

Two systems with one complex plus 12 free BTP and 12 CMPO ligands were simulated in octanol–water binary mixtures (see Fig. 8). In the first one the complex was initially positioned at the interface of a "rectangular" box, and the free BTP and CMPO ligands were equally shared between the two phases. After 15 ns of dynamics, all hydrophobic ligands were forced out of water, and mainly diffused to the octanol phase where they are soluble, whereas the complex remained adsorbed at the interface for the whole dynamics, indicating that it is surface active.

The second simulation involved a more severe sampling, as it started with randomly mixed phases and solutes, and was performed with a cubic solvent box in order to keep the system as isotropic as possible. In fact, during the dynamics the phases separated as in the neat solvent mixture to form an octanol bilayer and a water slab (Fig. 8). The resulting interfacial area is *ca.* 1.6 times larger than in the system simulated from juxtaposed phases, but the distribution of solutes is qualitatively similar: the majority of ligands are diluted in the octanol phase, the complex is anchored at the

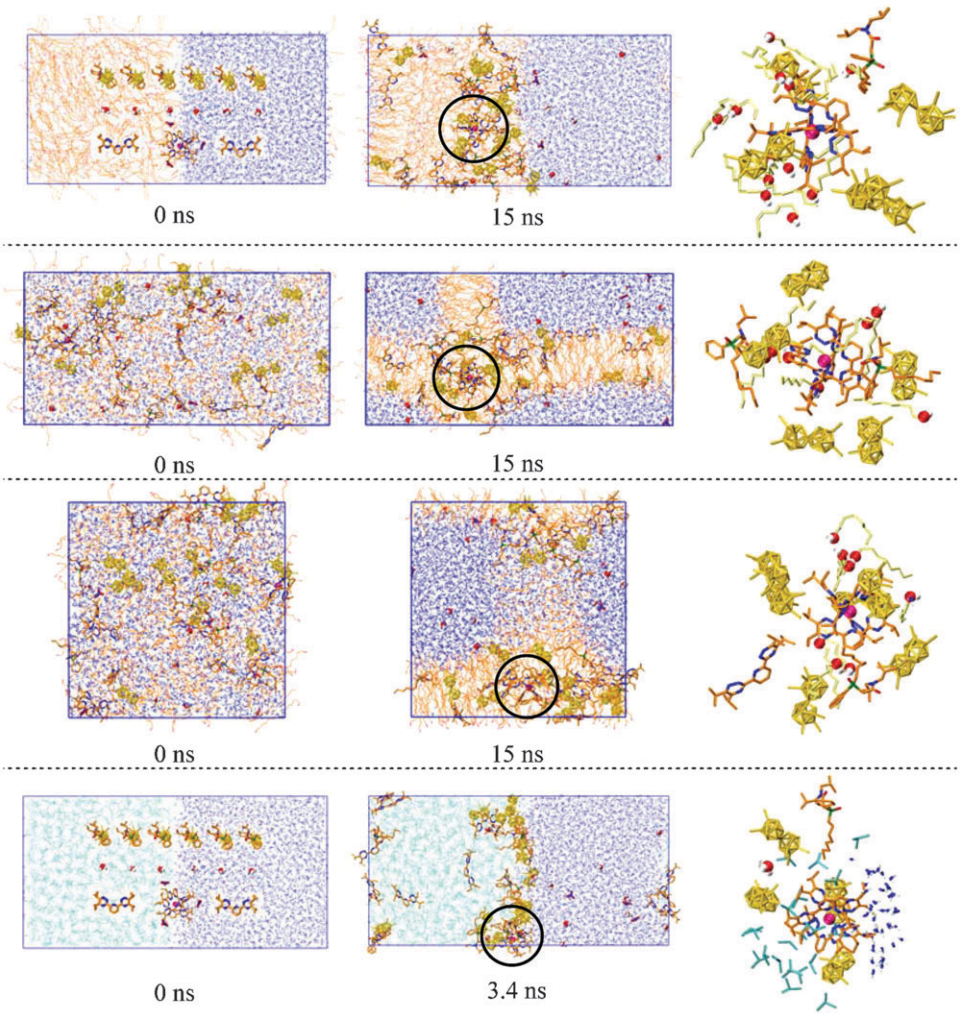

Fig. 9 The $Eu(BTP)_3^{3+}$, 3 NO_3^- complex in the presence of 12 CMPO and 12 BTP ligands plus 12 CCD^- H_3O^+ ions. From top to bottom: the octanol–water interface, simulated from juxtaposed liquids (top), from mixed liquids in a rectangular box (middle), or in a cubic box (bottom), and the chloroform–water interface. Initial and final views, with typical snapshots of the $Eu(BTP)_3^{3+}$ complex "extracted" to the octanol phase, or adsorbed at the chloroform interface. More detailed representations of the final systems are given in Fig. S12.†

interface, whereas the hydrophilic NO_3^- counterions sit in the water slab. Thus, although Eu^{3+} is shielded from water by the ligands, its $Eu(BTP)_3^{3+}$ complex is not extracted. The main reason comes from medium and long range charge dipole interactions between the +3 cation and water molecules, as seen from the zoomed snapshots in Fig. 8, and from the high interaction energy of the complex and water (*ca.* −185 and −140 kcal mol^{-1}, respectively in the juxtaposed and demixed systems).

2. Synergistic effect of CCD^- upon extraction of Eu^{3+} ions to octanol

The effect of CCD^- is clearly seen from simulations on the same biphasic systems as above (containing one $Eu(BTP)_3^{3+}$ complex plus 12 CMPO and 12 BTP molecules) to which 12 CCD^-, H_3O^+ ions were added, starting either from juxtaposed or from "randomly mixed" liquids. Typical snapshots at the beginning and at the end (15 ns) of dynamics are presented in Fig. 9 and Fig. S12.†

During the simulation of juxtaposed liquids, starting with the complex at the interface and the other species equally shared between the two phases, all ligands and CCD^- anions were driven out of the water. The majority concentrated on the octanol side of the interface, and attracted the Eu^{3+} complex that completely quit the interface. As seen on a snapshot (Fig. 9), there is no water within *ca.* 10 Å from the Eu^{3+} cation which is surrounded by the three BTP ligands, *ca.* 5 CCD^- anions, 10 octanol molecules, plus 1 to 3 remote CMPO and BTP ligands, and can thus be considered as "extracted". The total interaction energy between the complex and water becomes somewhat repulsive (+20 kcal mol^{-1}), in contrast to what was found without the CCD^-'s. Looking at the total charge of the "bulk" octanol phase, it is found to be nearly neutral as in the case of the CCD^- Cs^+ salt, as the organic phase contains *ca.* 8 negative charges (7 CCD^- plus 1 NO_3^- anions) and 7 positive charges (4 H_3O^+ and the Eu^{3+} complex) on average, during the last 0.7 ns.

As in the case of the neat solvent mixture, the demixing simulation of the "randomly mixed" system led to the

formation of octanol bilayers and, most importantly, the complex sits right at the crossing between the "horizontal" and "vertical bilayer (see Fig. 9), in a hydrophobic octanol environment. As seen in Fig. 9, CCD^-'s play a key role in solubilizing the complex in the octanol microphase, as *ca.* 5 of them sit within 10 Å from the cation. The complex is thus mainly surrounded by CCD^- and octanol molecules. The majority of free BTP and CMPO ligands are inserted in the bilayer structure (Fig. S12).† The former are most hydrophobic and display rare contacts with water, whereas the CMPO's are more amphiphilic and tend to adsorb at the interface.

We again performed another mixing–demixing simulation on the same system, but in a cubic, instead of elongated solvent box, which, unsurprisingly, might somewhat prevent the formation of an elongated octanol bilayer. The resulting final state (at 15 ns) represented in Fig. 9 confirms that the water and octanol phases are separated, but less than they were with an elongated box. One can see a big domain where water and octanol molecules remain mixed. In fact, due to the confined size of the box, these octanol molecules can hardly be inserted into the formed bilayer, thereby preventing water to condense into a single bulk phase. The most important feature, however, concerns the $Eu(BTP)_3^{3+}$ complex that is again fully extracted to the octanol microphase, without any contact with the aqueous interface. As in the two other systems, it is surrounded by an "anionic cage" of 5 CCD^- and by octanol molecules, plus transient free BTP ligands.

Experimentally, there is an equilibrium between complexed and uncomplexed ligands plus, in some cases, other extractant molecules (*e.g.* diamides, tri-*n*-butylphosphate TBP, CMPO) that are added in order to presumably co-complex the cation. An excess of ligands also shifts the complexation equilibrium towards high ligand : metal stoichiometries, rendering the complex more hydrophobic and more extractable. As seen in the present and other simulations,[53,57,75–77] the added ligands also display surface activity (see also experimental data),[78] thereby reducing the interfacial pressure and facilitating the interface crossing by the complex. In the case of the simulated cation extraction by BTP ligands, additional ligands, like BTP or CMPO, do not seem to play a key role in the extraction process of the $Eu(BTP)_3^{3+}$ complex, once formed. Indeed, repeating the same simulation as above with the complex and 12 CCD^-, H_3O^+ ions, but without CMPO and BTP ligands, shows that the complex is also extracted to octanol, as a result of its attractions with the CCD^-'s (Fig. S13).†

Dicussion and conclusions

We report a molecular dynamics investigation on the synergistic effect of dicarbollides anions upon extraction of the highly hydrophilic Eu^{3+} cation by BTP ligands to an octanol solution, with a main focus on the interfacial landscape in ion extraction. As shown by our simulations and others,[34,41,44,45] octanol is quite heterogeneous and thus displays dual solvation properties. Its polar OH head is involved in the solvation of moderately hard ions (*e.g.* Cs^+, NO_3^-), whereas its alkyl chain solvates soft hydrophobic anions like CCD^- that are therefore more soluble in this solvent than in chloroform or in aliphatic solvents. Their solubility is reflected in the simulations by the lack of condensation, which contrasts with the formation of hydrophobic anionic aggregates in water (confirmed by recent experiments),[79] and of amorphous neutral molten salts in chloroform. In octanol, there is some degree of CCD^- Cs^+ ion pairing, which should also presumably be the case for CCD^- H_3O^+ ions.

Octanol is also an amphiphile and forms, at aqueous interfaces, an ordered layer. Our simulations correspond to liquids confined in a "nanoscopic box" represented with 3D-periodic boundary conditions and the structure of octanol behind that interfacial layer depends on the size and shape of the system, and on the octanol : water ratio. We see cases where the "bulk" octanol phase beyond the interface is rather isotropic as in the neat liquid, and cases with a strongly ordered bilayer structure, in contact with water slabs.[80] It should be recalled the "demixing simulations" are, in fact, a mere "computational trick" used to avoid being trapped close to an initial potential well at the beginning of the dynamics. On the other hand, the fact that in the demixing simulations, water and octanol microphases separate in *ca.* 8 ns means that, in reality, these liquids at rest do not mix on a microscopic level, thereby emphasizing the importance of their mutual interface.

In the presence of bulky solutes like CCD^- anions, BTP and CMPO ligands, or the $Eu(BTP)_3^{3+}$ complex, octanol is less ordered at the interface and in the bulk domain, and its aggregation type (bilayer *versus* monolayer followed by an "isotropic" bulk phase) again depends on the starting situation and on the shape of the solvent box in the 50 : 50 mixtures. When water is in excess, octanol forms a spherical micelle, while octanol in excess solubilizes water and the CCD^- salts in its polar domains.

Whatever the simulation conditions, however, the CCD^-'s are found to be too hydrophobic to partition to the aqueous phase and thus prefer the octanol microphase where they are soluble. A large fraction (*ca.* 60%) adsorb at the interface, while others sit in "bulk" octanol, indicating they are less surface active at the octanol than at the chloroform interface.[20] On the other hand, the associated hydrophilic counterions (Cs^+, Eu^{3+}) are in excess on the aqueous side of the interface, creating an interfacial potential, negative on the octanol side, and positive on the water side of the interface. The CCD^-'s thus attract their counterions at the interface, or even in the octanol phase, in the form of weakly hydrated ion (Cs^+ case), or of fully hydrated ions (Eu^{3+} case). The more hydrophilic the cation, the highest amount of dragged water, possibly explaining why the free energies of transfer of Na^+, K^+, Rb^+ and Cs^+ dicarbollide salts from water to octanol are quasi-identical.[81]

Formally, cation complexes like $Eu(BTP)_3^{3+}$ behave like a big cation, and their interfacial behavior depends on the nature of the oil phase, and on the presence of CCD^- anions. In the absence of CCD^- anions, the complex adsorbs at the octanol, as well as chloroform interfaces with water. The driving forces for their surface activity are (i) the strong charge–dipole attractions between the charged complex and water and (ii) the high volume of the complex that tends to be driven out of water, in order to avoid paying the price of the cavity formation ("cavitation energy") in water [82] which is

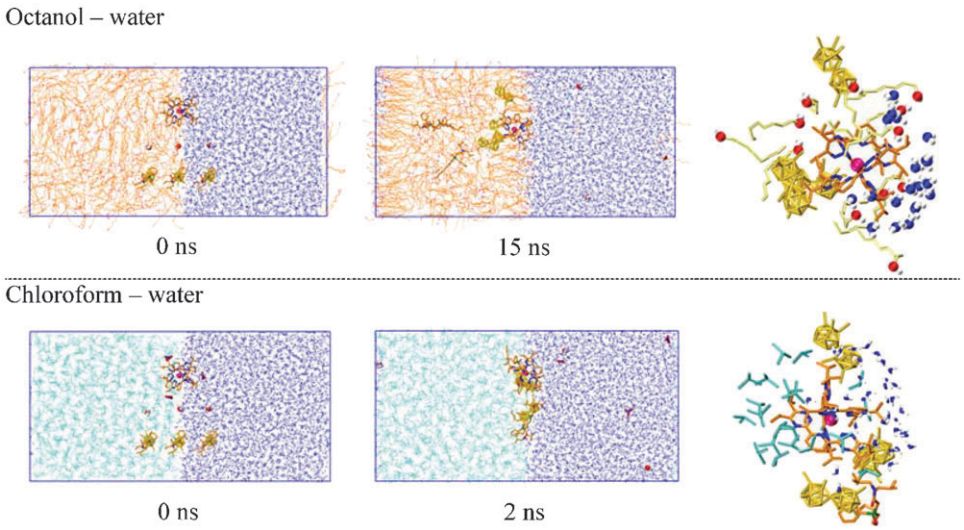

Fig. 10 The $Eu(BTP)_3^{3+}$, 3 NO_3^-complex in the presence of 3 CMPO ligands and 3 CCD^- H_3O^+ ions at the octanol–water and chloroform–water interfaces. Initial and final views of the solvent box and zoom of the $Eu(BTP)_3^{3+}$ complex adsorbed at the interface.

higher than in octanol (the difference would amount to *ca.* 1.5 kcal mol^{-1} for a spherical cavity of 5 Å radius).[83] Also, note that its counterions sit either in water (in the case of NO_3^- counterions), or at the interface (in the case of three CCD^- counterions per complex; see Fig. 10), where they attract the complex, thereby preventing its extraction towards the octanol of chloroform phases.

When an excess of CCD^- anions are added to the solution, they clearly promote the extraction of the $Eu(BTP)_3^{3+}$ complex to the octanol phase *via* "coulombic catalysis". The CCD^-'s concentrate locally and trap the complex inside an anionic "cage", thereby impeding its contacts with water. For that purpose, a large amount of CCD^-'s is needed, as demonstrated by a simulation of the $Eu(BTP)_3(NO_3)_3$ complex plus 3 CCD^- H_3O^+ and 3 CMPO ligands at the octanol–water and chloroform–water interfaces (Fig. 10). Formally, the complex might be extracted as a neutral $Eu(BTP)_3(CCD)_3$ species, but it is not and remains anchored at the interface. The 3 CCD^- anions also located at the interface, within *ca.* 10 Å from europium, but the $Eu(BTP)_3^{3+}$ moiety is clearly attracted by water (by −75 kcal mol^{-1}; also note that there are *ca.* 35 H_2O molecules within 10 Å from Eu^{3+}). A similar situation is found with chloroform as the organic phase (see Fig. 10), combining the higher surface activity of the CCD^- anions themselves and of the Eu^{3+} complex. Thus, stoichiometric proportions of CCD^-'s are not sufficient for promoting the extraction of the complex. A sufficiently large amount is needed to attract and extract the complex to the organic phase. When the organic phase poorly solubilizes the CCD^- anions, the latter condense at the interface and trap the complex in that domain, instead of extracting it to the oil phase, as in the case of chloroform–water system. In all cases, the exchange between the n CCD^- counterions (Cs^+ or H_3O^+) from the organic phase with the $+n$ charged cation from the aqueous phase is an important driving force for the extraction of M^{n+} cations, but is not sufficient for driving the extraction to, *e.g.*, aliphatic or halogenated solvents where CCD^-'s are poorly soluble.

Another difference between octanol and chloroform as the receiving phase in cation extraction concerns the solvation of the europium counterions. In fact, in our simulations at interfaces, no NO_3^- is extracted to chloroform, whereas one finds 1 to 2 NO_3^- anions in the octanol phase, well solvated by $H_{octanol}$ protons, co-extracted with Eu^{3+} in the presence of CCD^-'s, in conjunction with the dual solvation properties of octanol.

Basically, the simulation results point to the importance of counterions in cation extraction, and of the solvation properties of the receiving phase towards the latter. They also provide some clues on the effect of "solvent modifiers" used to improve the physical properties of the receiving phase and to co-extract anions.[84–86] "Synergistic effects" at liquid–liquid interfaces are not only relevant for ion extraction processes,[87] but also for other processes like phase transfer catalysis,[18] interfacial electrochemistry,[19,88] membrane crossing in biological systems[89] and interfacial nanochemistry.[90]

Acknowledgements

The authors are grateful to IDRIS, CINES, Louis Pasteur University, and PARIS for computer resources, and Etienne Engler for assistance. GC thanks the Louis Pasteur University for a PhD grant.

References

1 M. F. Hawthorne, D. C. Young and P. A. Wegner, *J. Am. Chem. Soc.*, 1965, **87**, 1818–1819.
2 J. Rais and B. Grüner, in *Ion Exchange Solvent Extraction*, ed. Y. Marcus, A. K. SenGupta and J. A. Marinsky, M. Dekker, New York, 2004, pp. 243–324.
3 V. N. Romanovski, I. V. Smirnov, V. A. Babain, T. A. Todd, R. S. Herbst, J. D. Law and K. N. Brewer, *Solvent Extr. Ion Exch.*, 2001, **19**, 1–21.
4 R. S. Herbst, J. D. Law, T. A. Todd, V. N. Romanovski, V. A. Babain, V. M. Esimantovskiy, I. V. Smirnov and B. N. Zaitsev, *Solvent Extr. Ion Exch.*, 2002, **20**, 429–445.
5 M. Kyrs, K. Svoboda, P. Lhotak and J. Alexova, *J. Radioanal. Nucl. Chem.*, 2002, **254**, 455–464.

6 M. Kyrs, K. Svoboda, P. Lhotak and J. Alexova, *J. Radioanal. Nucl. Chem.*, 2003, **258**, 497–509.
7 I. V. Smirnov, V. A. Babain, A. Y. Shadrin, T. I. Efremova, N. A. Bondarenko, R. S. Herbst, D. R. Peterman and T. A. Todd, *Solvent Extr. Ion Exch.*, 2005, **23**, 1–21.
8 M. Y. Alyapyshev, V. A. Babain and I. V. Smirnov, *Radiochemistry*, 2004, **46**, 270–271.
9 M. M. Reinoso-Garcia, W. Verboom, D. N. Reinhoudt, F. Brisach, F. Arnaud-Neu and K. Liger, *Solvent Extr. Ion Exch.*, 2005, **23**, 425–437.
10 B. Grüner, J. Plesek, J. Baca, J. F. Dozol, V. Lamare, I. Cisarova, M. Belohradsky and J. Caslavsky, *New J. Chem.*, 2002, **26**, 867–875.
11 B. Grüner, J. Plesek, J. Baca, I. Cisarova, J. F. Dozol, H. Rouquette, C. Vinas, P. Selucky and J. Rais, *New J. Chem.*, 2002, **26**, 1519–1527.
12 J. Rais, S. Tachimori, P. Selucky and K. Kadlecova, *Sep. Sci. Technol.*, 1994, **29**, 261–274.
13 C. Vinas, S. Gomez, J. Bertran, F. Teixidor, J. F. Dozol and H. Rouquette, *Chem. Commun.*, 1998, 191–192.
14 J. F. Dozol, V. Boehmer, A. Mckervey, F. Lopez-Calahorra, D. Reinhoudt, M. J. Schwing, R. Ungaro and G. Wipff, *European Commission, Directorate General Science, Research and Development, Contract No. F12W-CT-0062, Final report, EUR17615 EN*, 1997.
15 A. Popov and T. Borisova, *J. Colloid Interface Sci.*, 2001, **236**, 20–27.
16 C. Hill and B. Grüner, *EUROPART European Project on Partitioning*, 2006.
17 C. Hansch and W. J. Dunn, *J. Pharm. Sci.*, 1972, **61**, 1–19.
18 C. M. Starks, C. L. Liotta and M. Halpern, in *Phase Transfer Catalysis*, ed. C. M. Starks, Chapmann & Hall, New York, 1994.
19 H. H. Girault and D. J. Schiffrin, in *Electroanalytical Chemistry*, ed. A. J. Bard, Dekker, New York, 1989, pp. 1–141, and references cited therein.
20 G. Chevrot, R. Schurhammer and G. Wipff, *J. Phys. Chem. B*, 2006, **110**, 9488–9498.
21 Z. Kolarik, U. Müllich and F. Gassner, *Solvent Extr. Ion Exch.*, 1999, **17**, 23–32.
22 M. G. B. Drew, D. Guillaneux, M. J. Hudson, P. B. Iveson, M. L. Russell and C. Madic, *Inorg. Chem. Commun.*, 2001, **4**, 12–15.
23 M. A. Denecke, A. Rossberg, P. J. Panak, M. Weigl, B. Schimmelpfennig and A. Geist, *Inorg. Chem.*, 2005, **44**, 8418–8425.
24 M. Weigl, A. Geist, U. Mullich and K. Gompper, *Solvent Extr. Ion Exch.*, 2006, **24**, 845–860.
25 C. Madic, M. Lecomte, P. Baron and B. Boullis, *C. R. Phys.*, 2002, **3**, 797–811.
26 L. H. Delmau, T. J. Lefranc, P. V. Bonnesen, J. C. Bryan, D. J. Presley and B. A. Moyer, *Solvent Extr. Ion Exch.*, 2005, **23**, 23–57.
27 J. Szymanowski, G. Cote, I. Blondet, C. Bouvier, D. Bauer and J. L. Sabot, *Hydrometallurgy*, 1997, **44**, 163–178.
28 A. Heyberger, J. Prochazka and E. Volaufova, *Chem. Eng. Sci.*, 1998, **53**, 515–521.
29 B. Abecassis, F. Testard, T. Zemb, L. Berthon and C. Madic, *Langmuir*, 2003, **19**, 6638–6644.
30 J. Sangster, in *Octanol–water Partition Coefficients: Fundamentals and Physical Chemistry*, ed. P. T. G. Fogg, Wiley Series in Solution Chemistry, J. Wiley, Chichester, 1997.
31 D. T. Cramb and S. C. Wallace, *J. Phys. Chem. B*, 1997, **101**, 2741–2744.
32 G. G. Briggs, *J. Agric. Food Chem.*, 1981, 1050–1059.
33 R. A. Dobbs, W. Leping and G. Rakesh, *Environ. Sci. Technol.*, 1989, 1092–1097.
34 S. E. DeBolt and P. A. Kollman, *J. Am. Chem. Soc.*, 1995, **117**, 5316–5340.
35 S. A. Best, J. K. M. Merz and C. H. Reynolds, *J. Phys. Chem. B*, 1999, **103**, 714–726.
36 B. Chen and J. I. Siepmann, *J. Am. Chem. Soc.*, 2000, **122**, 6464–6467.
37 C. A. de Oliveira, C. R. W. Guimaraes and R. B. de Alencastro, *Int. J. Quantum Chem.*, 2002, **90**, 786–791.
38 J. L. MacCallum and D. P. Tieleman, *J. Am. Chem. Soc.*, 2002, **124**, 15085–15093.
39 B. Chen and J. I. Siepmann, *J. Phys. Chem. B*, 2006, **110**, 3555–3563.
40 $\eta_{octanol}$ = 7.29; $\eta_{chloroform}$ = 0.54; η_{water} = 0.89 mPa s at 298 K See: *Handbook of Chemistry and Physics*, CRC Press, Boca Raton, FL, 78th edn, 1997–1998.
41 R. L. Napoleon and P. B. Moore, *J. Phys. Chem. B*, 2006, **110**, 3666–3673.
42 D. Michael and I. Benjamin, *J. Phys. Chem.*, 1995, **99**, 16810–16813.
43 D. Michael and I. Benjamin, *J. Chem. Phys.*, 2001, **114**, 2817–2824.
44 I. Benjamin, *Chem. Phys. Lett.*, 2004, **393**, 453–456.
45 J. W. Lambert and A. K. Sum, *J. Phys. Chem. B*, 2006, **110**, 2351–2357.
46 H. Watarai, *Trends Anal. Chem.*, 1993, **12**, 313–318.
47 D. A. Case, D. A. Pearlman, J. W. Cadwell, T. E. Cheatham III, J. Wang, W. S. Ross, C. L. Simmerling, T. A. Darden, K. M. Merz, R. V. Stanton, A. L. Cheng, J. J. Vincent, M. Crowley, V. Tsui, H. Gohlke, R. J. Radmer, Y. Duan, J. Pitera, I. Massova, G. L. Seibel, U. C. Singh, P. K. Weiner and P. A. Kollman, *AMBER7*, University of California, San Francisco, 2002.
48 D. G. De Boer, A. Zalkin and D. H. Templeton, *Inorg. Chem.*, 1968, **7**, 2288.
49 B. Coupez and G. Wipff, *C. R. Chim.*, 2004, **7**, 1153–1164.
50 M. Dolg, H. Stoll, A. Savin and H. Preuss, *Theor. Chim. Acta*, 1989, **75**, 173–194.
51 M. Dolg, H. Stoll, A. Savin and H. Preuss, *Theor. Chim. Acta*, 1993, **85**, 441–450.
52 G. W. Trucks, H. B. Schlegel, G. E. Scuseria, M. A. Robb, J. R. Cheeseman, J. A. Montgomery, Jr, T. Vreven, K. N. Kudin, J. C. Burant, J. M. Millam, S. S. Iyengar, J. Tomasi, V. Barone, B. Mennucci, M. Cossi, G. Scalmani, N. Rega, G. A. Petersson, H. Nakatsuji, M. Hada, M. Ehara, K. Toyota, R. Fukuda, J. Hasegawa, M. Ishida, T. Nakajima, Y. Honda, O. Kitao, H. Nakai, M. Klene, X. Li, J. E. Knox, H. P. Hratchian, J. B. Cross, C. Adamo, J. Jaramillo, R. Gomperts, R. E. Stratmann, O. Yazyev, A. J. Austin, R. Cammi, C. Pomelli, J. W. Ochterski, P. Y. Ayala, K. Morokuma, G. A. Voth, P. Salvador, J. J. Dannenberg, V. G. Zakrzewski, S. Dapprich, A. D. Daniels, M. C. Strain, O. Farkas, D. K. Malick, A. D. Rabuck, K. Raghavachari, J. B. Foresman, J. V. Ortiz, Q. Cui, A. G. Baboul, S. Clifford, J. Cioslowski, B. B. Stefanov, G. Liu, A. Liashenko, P. Piskorz, I. Komaromi, R. L. Martin, D. J. Fox, T. Keith, M. A. Al-Laham, C. Y. Peng, A. Nanayakkara, M. Challacombe, P. M. W. Gill, B. Johnson, W. Chen, M. W. Wong, C. Gonzalez and J. A. Pople, *M. J. F. GAUSSIAN 03, (Revision B.05)*, Gaussian Inc., Pittsburgh PA, 2003.
53 P. Guilbaud and G. Wipff, *New J. Chem.*, 1996, **20**, 631–642.
54 J. Aqvist, *J. Phys. Chem.*, 1990, **94**, 8021–8024.
55 F. C. J. M. van Veggel and D. N. Reinhoudt, *Chem.–Eur. J.*, 1999, **5**, 90–95.
56 W. L. Jorgensen, J. Chandrasekhar, J. D. Madura, R. W. Impey and M. L. Klein, *J. Phys. Chem.*, 1983, **79**, 926.
57 N. Muzet, E. Engler and G. Wipff, *J. Phys. Chem. B*, 1998, **102**, 10772–10788.
58 H. J. C. Berendsen, J. P. M. Postma, W. F. van Gunsteren and A. Di Nola, *J. Chem. Phys.*, 1984, **81**, 3684.
59 E. Engler and G. Wipff, in *Cristallography of Supramolecular Compounds*, ed. G. Tsoucaris, Kluwer, Dordrecht, The Netherlands, 1996, p. 471.
60 W. Humphrey, A. Dalke and K. Schulten, *J. Mol. Graphics*, 1996, **14**, 33–38.
61 G. Wipff, E. Engler, P. Guilbaud, M. Lauterbach, L. Troxler and A. Varnek, *New J. Chem.*, 1996, **20**, 403–417.
62 M. P. Allen and D. J. Tildesley, in *Computer Simulation of Liquids*, ed. W. F. van Gunsteren and P. K. Weiner, Clarendon Press, Oxford, 1987.
63 *The Properties of Solvents*, ed. Y. Marcus, Wiley Series in Solution Chemistry, John Wiley & Sons, Chichester, 1998.
64 P. Sassi, M. Paolantoni, R. S. Cataliotti, F. Palombo and A. Moressi, *J. Phys. Chem. B*, 2004, **108**, 19557–19565.
65 N. Sieffert and G. Wipff, *J. Phys. Chem. B*, 2006, **110**, 13076–13085.
66 G. Chevrot, R. Schurhammer and G. Wipff, *Phys. Chem. Chem. Phys.*, 2006, **8**, 4166–4174.
67 W. H. Steel and R. A. Walker, *Nature*, 2003, **424**, 296–299.
68 W. H. Steel, C. L. Beildeck and R. A. Walker, *J. Phys. Chem. B*, 2004, **108**, 16107–16116.

69 The calculated diffusion coefficients are $D_{octanol} = 32.10^{-7}$ and $D_{chloroform} = 518.10^{-7}$ cm^2 s^{-1} in the biphasic systems and $D_{octanol} = 27.10^{-7}$ and $D_{chloroform} = 257.10^{-7}$ cm^2 s^{-1} in the pure liquids.
70 In order to further investigate the sampling issue and the possible interconversion between the final boxes obtained from the juxtaposed *versus* randomly mixed liquids, we pursued both dynamics for 5 additional nanoseconds at a higher temperature of 350 K to enhance the sampling. The two systems, however, retained their overall characteristics without undoing interconversions. Furthermore, the internal energy of the bilayer type demixed system remained lower (by 330 kcal mol^{-1}) than the energy of the system with juxtaposed liquids.
71 K. E. Wardle, E. Carlson, D. Henderson and R. L. Rowley, *J. Chem. Phys.*, 2004, **120**, 7681–7688.
72 V. Srinivasan and D. Blankschtein, *Langmuir*, 2003, **19**, 9946–9961.
73 V. Srinivasan and D. Blankschtein, *Langmuir*, 2003, **19**, 9932–9945, and references cited therein.
74 The Eu^{3+} cation is surrounded by *ca.* 30–40 H_2O molecules within 8.4 Å in the octanol phase. Within the same distance, there are *ca.* 70 H_2O molecules in the bulk water phase.
75 G. Wipff, E. Engler, P. Guilbaud, M. Lauterbach, L. Troxler and A. Varnek, *New J. Chem.*, 1996, **20**, 403–417.
76 F. Berny, N. Muzet, L. Troxler and G. Wipff, in *Supramolecular Science: where it is and where it is going*, ed. R. Ungaro and E. Dalcanale, Kluwer Academic Publishers, Dordrecht, 1999, pp. 95–125, and references cited therein.
77 M. Baaden, M. Burgard and G. Wipff, *J. Phys. Chem. B*, 2001, **105**, 11131–11141.
78 J. Szymanowski, *Solvent Extr. Ion Exch.*, 2000, **18**, 729–751.
79 P. Matejicek, P. Cigler, K. Prochazka and V. Kral, *Langmuir*, 2006, **22**, 575–589.
80 As an additional computational test, we simulated the water/octanol mixture of an identical composition (2048 H_2O plus 256 octanol molecules) as in the simulation of R. L. Napoleon and P. B. Moore (*J. Phys. Chem. B*, 2006, **110**, 3666), also starting with a ''random mixture''. Our results presented in Fig. S14 are different, as we clearly obtain bilayers, instead of ''juxtaposed liquids'' as reported by these authors. Our final box dimensions are $35 \times 35 \times 104$ A^3. Further methodological investigations are thus required to better understand these structures.
81 J. Rais, T. Okada and J. Alexova, *J. Phys. Chem. B*, 2006, **110**, 8432–8440.
82 R. A. Pierotti, *Chem. Rev.*, 1976, **76**, 717–726.
83 S. Höfinger and F. Zerbetto, *Theor. Chem. Acc.*, 2004, **112**, 240–246.
84 B. A. Moyer, in *Molecular Recognition: Receptors for Cationic Guests*, ed. J. L. Atwood, J. E. D. Davies, D. D. McNicol, F. Vögtle and J.-M. Lehn, Pergamon, New York, 1996, pp. 325–365, and references cited therein.
85 B. A. Moyer, P. V. Bonnesen, R. Custelcean, L. H. Delmau and B. P. Hay, *Kem. Ind.*, 2005, **54**, 65–87.
86 L. H. Delmau, T. J. Lefranc, P. V. Bonnesen, J. C. Bryan, D. J. Presley and B. A. Moyer, *Solvent Extr. Ion Exch.*, 2005, **23**, 23–57.
87 H. Watarai, K. Sasaki, K. Takahashi and J. Murakami, *Talanta*, 1995, **42**, 1691–1700.
88 W. Schmickler, *Interfacial Electrochemistry*, Oxford University Press, New York, 1996.
89 A. G. Volkov, D. W. Deamer, D. L. Tanelian and V. S. Markin, *Liquid Interfaces in Chemistry and Biology*, John Wiley & Sons, Inc., New York, 1998.
90 H. Watarai, N. Teramae and T. Sawada, in *Interfacial Nanochemistry. Molecular Science and Engineering at liquid–liquid Interfaces*, Nanostructure Science and Technology, ed. D. J. Lockwood, Kluwer Academic Plenum, New York, 2005.